Tropical Journal of Pharmaceutical Research February 2021; 20 (2): 389-401
ISSN: 1596-5996 (print); 1596-9827 (electronic)

Available online at http://www.tjpr.org
http://dx.doi.org/10.4314/tjpr.v20i2.25

Original Research Article

Rapid screening and characterization of caffeic acid metabolites in rats by UHPLC-Q-TOF mass spectrometry

Jiaqi Yuan[1], Yunting Wang[1], Shengquan Mi[1], Jiayu Zhang[2], Yaxuan Sun[1]*
[1]Beijing Key Laboratory of Bioactive Substances and Functional Foods, Beijing Union University, Beijing, [2]School of Pharmacy, Binzhou Medical University, Yantai 264003, China

For correspondence:* ***Email:* *sunxx@buu.edu.cn, msq65@buu.edu.cn;* ***Tel:*** *+86 010 62004604, +86 010 62004604*

Sent for review: 11 August 2020 *Revised accepted: 17 January 2021*

Abstract

Purpose: *To determine the metabolism of caffeic acid in rats.*
Methods: *Sprague-Dawley rats were intragastrically administered caffeic acid in saline suspension, and biological samples collected. After sample pretreatment by solid phase extraction, ultra-high performance liquid chromatography combined with quadrupole-time of flight mass spectrometry system (UHPLC-Q-TOF-MS/MS) was established to rapidly screen and characterize caffeic acid metabolites in rats. Waters HSS T3 UPLC chromatographic column (2.1 mm × 100 mm, 1.7 μm) was applied for the gradient elution with aqueous solution of formic acid (A)-acetonitrile (B). Mass spectral data for the biological samples in electrospray positive and negative ion modes were collected and analyzed by SCIEX OS 1.3 workstation.*
Results: *Based on their precise molecular weights and multistage mass spectrometry cleavage information, caffeic acid and 21 metabolites in vivo were identified. The results demonstrate that the biotransformation of caffeic acid in vivo was mainly achieved via hydrogenation, hydroxylation, methylation, sulfonation, glucuronidation, acetylation, and composite reactions.*
Conclusion: *The metabolites and metabolic pathways of caffeic acid in rats have been rapidly elucidated, and its potential pharmacodynamics forms have been clarified. This provides a valuable and meaningful reference for the study of caffeic acid metabolites, biological activities, and its medicinal material basis in vivo.*

Keywords: *Caffeic acid, UHPLC-Q-TOF-MS/MS, Metabolic profiling*

Tropical Journal of Pharmaceutical Research is indexed by Science Citation Index (SciSearch), Scopus, International Pharmaceutical Abstract, Chemical Abstracts, Embase, Index Copernicus, EBSCO, African Index Medicus, JournalSeek, Journal Citation Reports/Science Edition, Directory of Open Access Journals (DOAJ), African Journal Online, Bioline International, Open-J-Gate and Pharmacy Abstracts

INTRODUCTION

Phenolic acids, defined as organic acid containing phenol ring, which have various biological activities [1-3]. Caffeic acid (CA) is a kind of phenolic acids named also called 3, 4-dihydroxycinnamic acid (Figure 1), which has been proved that CA effectively alleviate oxidative stress [4]; reduce tumor cell viability [5,6]; inhibit the NF-κB signaling pathway and secretion of inflammatory factors [7-9]; ameliorate hippocampal neuron damage [10,11]. Altogether, CA has various biological activities and important research value. Li *et al* detected that CA had high bioavailability, fast metabolism, and could be sufficiently absorbed and utilized in rats [12]. However, there are no comprehensive

researches with the metabolic transformation and pathways of CA *in vivo*, which is very important to reveal the pharmacologically activities substances.

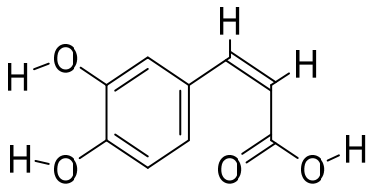

Figure 1: The structure of caffeic acid ($C_9H_8O_4$, *viz,* 3, 4-dihydroxycinnamic acid)

Ultra-high-performance liquid chromatography combined with high resolution mass spectrometry (UHPLC- HRMS) is one of the most universal techniques to study the chemical composition and content of food, the pharmacokinetics and metabolism of monomers in tradition Chinese medicines [13,14]. Quadrupole-time of flight mass spectrometry system (Q-TOF MS) has high precision, high sensitivity, fast qualitative analysis, good specificity, and ions relative intensity stability, has been widely used. [15-17]. Our study utilized UHPLC-Q-TOF MS/MS to explore the metabolism of CA in rats, to identify its metabolites and metabolic pathways *in vivo* and lays the foundation for research on biochemical transformation and mechanism of action of CA.

EXPERIMENTAL

Materials and reagents

ExionLC™ AC ultra-high performance liquid chromatography system (AB SCIEX, USA); SCIEX X500R Q-TOF mass spectrometer (AB SCIEX, USA) with heated electrospray source ion (HESI) and SCIEX OS 1.3 workstation; Waters HSS T3 UHPLC chromatographic column with specifications of 2.1 mm × 100 mm, 1.7 micron; Milli-Q Synthesis ultrapure water purification system (Millipore, USA); R200D electronic analytical balance (1/100,000) (Sartorius, Germany); KQ-250DE CNC ultrasonic cleaner (Kunshan ultrasonic instrument Co., Ltd.). CA with purity above 98 % was obtained from Biopurify Phytochemicals Ltd. (Chengdu, Sichuan, China) and applied to UHPLC-Q-TOF MS analysis. Formic acid (chromatography pure, Merck Company, Germany); Methanol and acetonitrile (mass spectrometry, Thermo Fisher, USA).

Six male Sprague Dawley (SD) rats approximately 220 g were purchased from Beijing Vital River Lab Animal Technology Co., Ltd. (Beijing, China). Animals were acclimatized for a week with water and free food intake, 12 h bright and dark cycle before the experiment. The environmental was quiet to prevent noise, and conditions were controlled at the temperature between 23 and 26 ℃, relative humidity of 50-65 %.

Sample collection and preparation

First, rats were randomized into the control group (n=3) and the drug group (n = 3). After fasting for 12 h, the rats were placed in metabolic cages during the experiment with free access to water. 180 mg CA was completely dissolved in 8 mL physiological saline and stored at 4 ℃. Drug group rats were given 200 mg/kg CA orally, while control group rats received equivalent saline. To allow the drug to accumulate and be better metabolized *in vivo*, we chose the continuous administration lasted for two days, one time per day.

The following methods were used to collect the complete metabolites of CA in the plasma within 4 h. A volume (0.5 mL) of blood of rats in drug group was taken from retro-orbital at 0.5 h, 1 h, 2 h and 4 h from the last gavage, and collected in an EP containing 10 μL of heparin sodium anticoagulant, allowed to left for 15 min followed by centrifuging for 10 min at 3,500 rpm. The resulting supernatants following centrifugation of blood samples of the drug group at each time point were collected and combined into one to produce a test plasma sample containing CA and stored at -80 ℃. Metabolism cages were used to collect 24 h later urine and feces samples after the last gavage. Centrifuged the urine samples for 10 min at 4 ℃, 3,500 rpm, and stored the supernatant at -80 ℃. The feces were dried in the fume hood, crushed and stored in the centrifugal tubes at -80 ℃. The blank samples were derived from control group rats, and collected and stored in the same way as the test samples.

Biological sample pretreatment

Sequentially with 3 mL methanol and 3 mL deionized water activated C_{18} solid phase extraction (SPE) columns. Thereafter, 1 mL plasma sample or urine sample allowed to unfreeze at room temperature was added into the SPE column respectively, followed by elution with 3 mL deionized water and 3 mL methanol. Finally, the methanol eluent was collected for N_2 blowing.

Deionized water was added to each feces sample in a ratio of 1:5 (w: v) and ultrasonically

extraction for 60 min. Then, centrifuged the supernatant for 10 min at 4 ℃, 3,500 rpm to obtain the blank feces and test feces sample. After activating the SPE columns, 2 mL of the supernatant from each feces sample was added. The impurities were washed with deionized water (3 mL) and methanol (3 mL) in sequence and collected the methanol extract.

At room temperature, all blood, urine and feces methanol eluents were dried by blowing nitrogen, then reconstituted the residues in 100 μL of 5 % acetonitrile, swirled for 3 min and centrifuged (14,000 rpm, 15 min) and collected supernatants to UPLLC-MS/MS for analysis.

Instruments and analytical conditions

The UHPLC-Q-TOF mass spectrometer was used for identifying CA metabolites. The chromatography was implemented on a Waters HSS T3UPLC chromatographic column with specifications of 2.1 mm × 100 mm, particle size 1.7 micron. After several optimization attempts, the mobile phase composed of 0.1 % formic acid (A) and acetonitrile (B)and the linear gradient optimization method described below: 0-6 min, 2-10 % A; 6-10 min, 10-25 % A; 10-15 min, 25-35 % A; 15-16 min, 35-40 % A; 16-20 min, 40-80 % A; 20-21 min, 80-95 % A; 21-24 min, 95-95 % A. The auto sampler temperature was set at 15 ℃ and chromatographic column 40 ℃. The elution flow rate was 0.3 mL/min under these conditions then loaded 10 μL.

MS was performance in the positive and negative ion modes. The optimized parameters were as below: HESI, 550 ℃, and 4.5 kV; auxiliary gas and sheath gas were high purity nitrogen (>99.99 % purity), 35 arb, and collision energy for 30 eV. The metabolites from *m/z* 100-1,500 were detected by full scanning MS analysis with a resolution of 70,000.

Data processing

The collected data was analyzed by SCIEX OS 1.3 workstation (AB SCIEX, USA). Metabolites were identified when the peaks intensity exceed 10,000 under ionization. Based on accurate measurement, taking into possible reactions and potential element composition, the types and quantity of elemental composition of compounds were set rang as below: C [0–20], H [0-35], O [0-15], S [0-3], N [0-3], and equivalent value of ring double bond [0-10]. The maximum errors between the theoretical mass to charge ratio and the experimental values were limited within 6 ppm.

RESULTS

Fragmentation behavior of CA under mass spectrometry

In positive ion mode, CA engendered the $[M+H]^+$ ion at *m/z* 181.0495 (Figure 2 A and B), which could be inferred to the molecular formula is $C_9H_8O_4$ (-0.2 ppm). The characteristic ions in the ESI-MS^2 spectrum of *m/z* 163.0392, *m/z* 152.0636, *m/z* 145.0281, *m/z* 135.0442, *m/z* 117.0334, and *m/z* 107.0494 were engendered by neutral loss filtering's (NLFs) of H_2O, CO, $2H_2O$, CO + H_2O, CO + $2H_2O$ and CO_2+CH_2O, respectively (Figure 2 C and D).

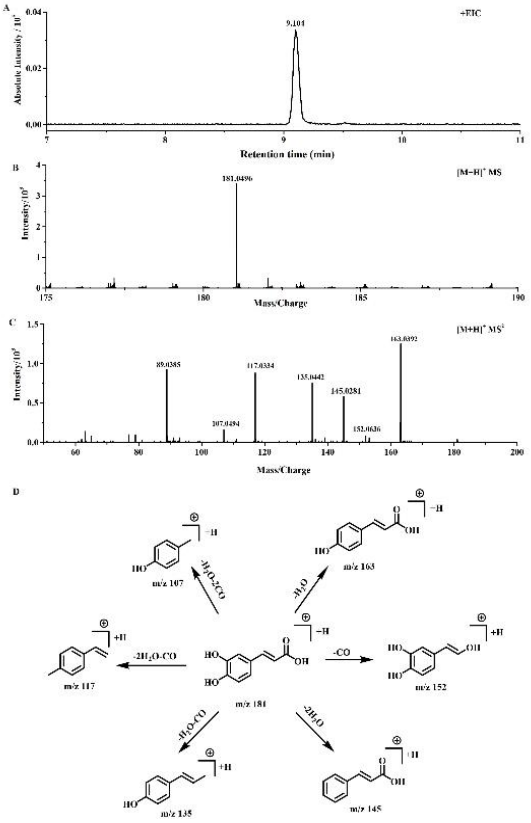

Figure 2: HESI-MS/MS spectrum of CA in positive ion mode, including the extract ion current chromatogram (EIC) (A), ESI-MS spectrum (B) and ESI-MS^2 spectrum (C) of CA, Fragmentation behavior of CA in MS^2 (D)

Meanwhile, CA engendered a *m/z* 179.0339 $[M-H]^-$ ion (Figure 3 A), which could be inferred to the molecular formula is $C_9H_8O_4$ (mass error -0.2 ppm) at 9.02 min (Figure 3 B). And the loss of CO_2 created the special fragments at *m/z* 135.0444 and *m/z* 134.0372 (Figure 3 C) in the ESI-MS^2 spectrum.

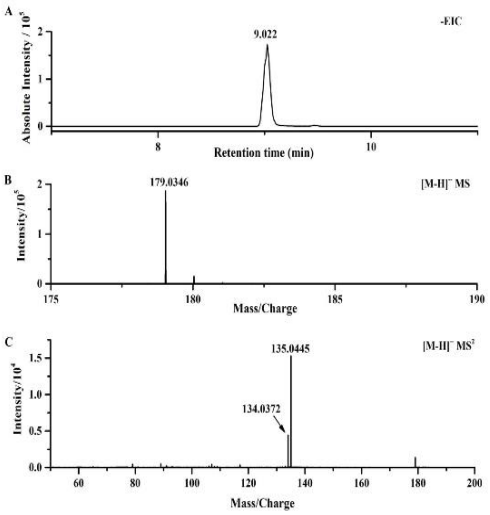

Figure 3: HESI-MS/MS spectrum of CA, including EIC (A), ESI-MS spectrum (B) and ESI-MS/MS spectrum (C) in negative ion mode

Identification of CA metabolites in rats

The UHPLC-Q-TOF-MS/MS system was applied for characterization of CA metabolites. Figure 4 shows the extract ion current chromatograms (EICs) of 21 metabolites about CA in positive and negative modes.

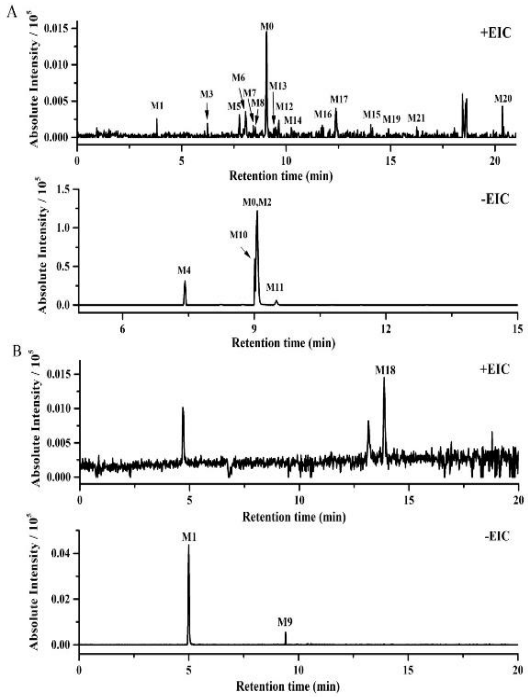

Figure 4: High-resolution EICs of metabolites in urine sample (A) and plasma sample (B) of drug rats

The urine, feces and plasma samples dates of the experimental rats after intragastric CA were collected and analyzed by SCIEX OS 1.3 workstation. By comparing the samples of the drug group and blank group, 22 metabolites were screened and identified as **M0** to **M21**. Figure 5 shows the proposed metabolic pathways of CA and Table 1 summarizes the relevant data on metabolites.

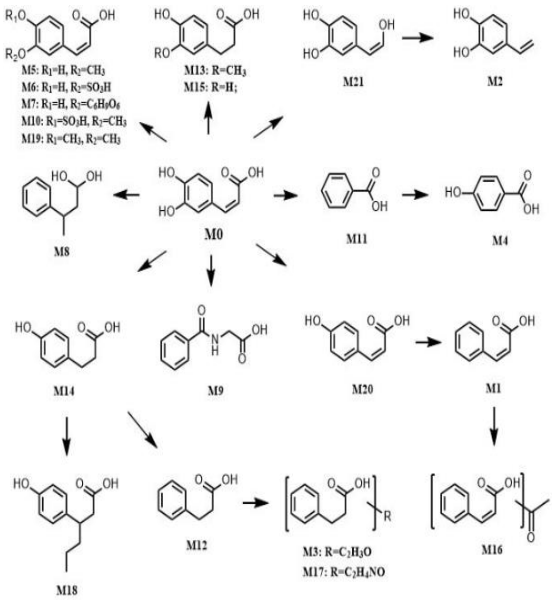

Figure 5: Proposed metabolic pathways of CA in rats

By comparing the relevant information with standard CA, **M0** was deduced as the drug prototype. The exact mass weight and characteristic ions (*m/z* 163, *m/z* 153, *m/z* 137, and *m/z* 135) of **M0** were identical with CA. **M1**, **M16**, and **M20** were eluted at 4.542, 11.334 and 15.170 min, respectively. Based on their characteristic fragment ions in the MS^2 spectra, we speculated that they have the same cinnamon group. **M20** exhibited its protonated molecular ion at *m/z* 165.0546 ($C_9H_8O_3$, error with 0.5 ppm) or *m/z* 163.0399 $[M-H]^-$ ($C_9H_8O_3$, error with 2.0 ppm). The ion at *m/z* 165 produced specific ions at *m/z* 137, *m/z* 123 and *m/z* 109 because of the successive loss of CO, C_2H_2O and C_2H_2O in its positive MS^2 spectrum, which aided us to preliminarily presume that it was dehydroxylation products of CA; in the negative MS^2 spectrum of **M20** was observed the NLFs of 46 Da and 16 Da (*m/z* 163→*m/z* 117→*m/z* 101), which occurred with the neutral loss $CO+H_2O$ and dihydroxylation, provided ample evidences for our inference. Therefore, **M20** was identified as the *p*-hydroxy-cinnamic acid. Then, we found that **M1** generated the $[M+H]^+$ ion at *m/z* 149.0597 ($C_9H_8O_2$, 1.0 ppm), which was 32 Da less than CA and 16 Da lower than **M20**, and

$[M+H-H_2O]^+$ at *m/z* 131 and $[M+H-CO_2]^+$ at *m/z* 105 were existed under ionization, which indicated that it was the dehydroxylation product of **M20** and twice dehydroxylation product of CA. And thus, we inferred that **M1** was Cinnamic acid. Again, we continued to analyze the $[M+H]^+$ ion peak of **M16** at *m/z* 191.0703 ($C_{11}H_{10}O_3$, -1.9 ppm), which was 42 Da higher than **M1**. Accordingly, the *m/z* 191 ion produced characterize ions at *m/z* 163 and 132 due to the successive loss of CO and CH_3, and the *m/z* 121 $[M+H-CH_2CO]^+$ illustrated that **M16** has an acetyl group. In view of the molecular formula and characteristic fragments, we conjectured **M16** was cinnamic acid acetylate.

Metabolite **M2** appeared at 5.443 min with a deprotonated ion at *m/z* 135.0451 ($C_8H_8O_2$, 1.0 ppm), and 44 Da lower than CA. **M2** were disintegrated $[M-H-H_2O]^-$ and $[M-H-CO]^-$ (*m/z* 135→*m/z* 107→*m/z* 89) under ionization, which identified that it was 1,2-hydroxy-4-vinylbenzene and the decarboxylate product of CA. Similarly, we found M21 produced the protonated ion at *m/z* 153.0546 $[M+H]^+$ ($C_8H_8O_3$, 0.5 ppm) at 16.495 min, which was 28 Da less than that of M0 and 16 Da more than that of **M2.** Its MS/MS spectra showed the $[M+H-CH_3]^+$ at *m/z* 138 and $[M+H-CO_2]^+$ at *m/z* 109. As a result, **M21** was presumed as the decarboxylation product as CA and the dehydroxylation product of **M2**.

According to the link between their characteristic ion at *m/z* 151 and CA, **M3** and **M17** were inferred to have the same phenylpropionic acid group. At 6.245 min, **M3** engendered its protonated ion at *m/z* 208.0968 ($C_{11}H_{13}NO_3$, 0.4 ppm) and *m/z* 206.0817 $[M-H]^-$ ($C_{11}H_{13}NO_3$, 1.6 ppm). It was 57 Da more than that of 3-phenylpropanoic acid (**M12**), and lost glycine and CO_2 molecule to generate *m/z* 151 and *m/z* 107, indicating it was the combination of 3-phenylpropionic acid and glycine. Then, at 12.149 min, **M17** engendered $[M+H]^+$ at *m/z* 193.0859 ($C_{11}H_{12}O_3$, -1.1 ppm). Due to consequent loss of CO and H_2O, the characteristic ion at *m/z* 193 was disintegrated the specific ion at *m/z* 147, and the diagnostic product ion (DPI) at *m/z* 151 $[M+H-Ac]^+$ was generated by loss of acetyl group. Hence, we deemed **M17** was 3-phenylpropionate acetylate.

At 5.443 min, **M4** provided $[M-H]^-$ ion at *m/z* 137.0244 ($C_7H_6O_3$, 4.5ppm). The characteristic ion at *m/z* 93 was produced by the loss of CO_2 with no other specific ions observed. Therefore, it was deduced as the *p*-hydroxybenzoic acid. **M11** was eluted at 9.304, 16 Da less than **M4**, showed a deprotonated ion at *m/z* 121.0295 ($C_7H_6O_2$, -2.1 ppm). The feature of fragment ion at *m/z* 93 through loss of CO in negative MS^2 spectrum, and the $[M-H-CO]^-$ ion at *m/z* 95 and *m/z* ion at 77 $[M-H-CO-H_2O]^-$were created in positive mode, which provide reliable basis for the identification of metabolite **M11**. According to the above data, we suspected it was benzoic acid and the structure of **M11** is as shown in Table 1, Table 2, Table 3 and Table 4. Due to the larger molecular structure of **M11**, the retention time in reversed-phase (RP) chromatography system was longer than **M4**. From their molecular formula structure and fragment ions in ESI-MS^2, we inferred that **M5**, **M6**, **M7**, **M10** and **M19** had a common cinnamic acid group. **M5** yielded $[M+H]^+$ ion at *m/z* 195.0653 ($C_{10}H_{10}O_4$, -1.0 ppm) at 7.752 min, which was 15 Da more than CA, indicating it was ferulic acid, the methylation product of CA. Its fragments $[M+H-CH_2]^+$ ion at *m/z* 180 and $[M+H-CH_2-CO_2]^+$ ion at *m/z* 136 were existed, which provide reliable evidence for our conclusion. At 8.255 min, **M6** was 80 Da more than CA and generated $[M-H]^-$ ion at *m/z* 258.9918 ($C_9H_8O_7S$, -5.8 ppm). The continuous NLFs of 80 Da and 44 Da (*m/z* 259→*m/z* 179→*m/z* 135) were existed, which indicated the sulfated metabolite of CA. **M7** with retention time of 7.752 min produced $[M-H]^-$ ion at *m/z* 355.0671 ($C_{15}H_{16}O_{10}$, -0.8 ppm) which was 176 Da more than CA, explaining that this may be a glucuronidation product of CA with the characteristic ions at *m/z* 179 and *m/z* 135 providing sufficient evidence for our deduction. **M10** exhibited a deprotonated ion at *m/z* 273.0064 ($C_{10}H_{10}O_7S$, 0.9 ppm) at 9.039 min and was 95 Da more than CA. The fragments at *m/z* 193, 178 and 134 were respectively generated by the NLFs of SO_3, SO_3+CH_3 and $SO_3+CH_3+CO_2$ and thus, it was putatively extrapolated as the sulfonation product of CA. **M19** exhibited a deprotonated at *m/z* 207.0652 $[M-H]^-$ ($C_{11}H_{12}O_4$, 0.1 ppm) at 14.907 min, which was 28 Da more than CA. Its MS^2 spectra showed the fragments at *m/z* 179, 135 and 161 were generated by loss of C_2H_4, $C_2H_4+CO_2$ and CO_2+ **H_2O**. Therefore, it was not hard to infer that M19 was the demethylation product of CA, and it was tentatively identified as 3,4-dimethoxycinnamic acid.

M8, eluted at 8.530 min possessed a protonated ion at *m/z* 167.0703 ($C_{10}H_{14}O_2$, error with 0.3 ppm). The ions at *m/z* 123, 109 and 91 were yielded by loss of CO_2, $C_2H_2O_2$ and CO_2+CH_4O in its ESI-MS/MS spectrum, so we suspected that it was 2-methyl-4-hydroxy-phenylpropionic acid. **M9** possessed the $[M-H]^-$ ion at *m/z* 178.0499 ($C_9H_9NO_3$, 1.3 ppm) at 9.407 min. The fragments at *m/z* 134 engendered through loss of CO_2 with no other specific fragment ions observed in MS^2 spectra, suggesting it might be hippuric acid, which exists in large amounts in

the urine of horses and other herbivores and in small amounts in human urine [18].

M12 engendered $[M+H]^+$ ion at *m/z* 151.0754 (C9H10O2, 0.3 ppm) at 9.405 min and 30 Da less than CA. Its characteristic fragment $[M+H-CO_2]^+$ ion at *m/z* 123 was existed, reason out **M12** could be 3-phenylpropanoic acid. **M14** was 16 Da more than **M12**, and presented the *m/z* 165.0546 $[M-H]^-$ ($C_9H_{10}O_3$, 1.1 ppm) at 10.735 min. In negative MS^2 spectrum, *m/z* 165 engendered characteristic ions at *m/z* 121, 119, and 106 through loss of CO_2, H_2O+CO, and CO_2+CH_3, respectively. Its positive MS^2 spectrum had the same results: fragments $[M+H-H_2O]^+$ at *m/z* 149 and $[M+H-CO]^+$ at *m/z* 121 were existed, suggesting that **M14** was *p*-hydroxybenzene propanoic acid.

M13 was 2 Da more than **M5**, and gave rise to its $[M-H]^-$ ion at *m/z* 195.0652 ($C_{10}H_{12}O_4$, 0.6 ppm) and $[M+H]^+$ ion at *m/z* 197.0808 ($C_{10}H_{12}O_4$, 2.9 ppm) . The NLFs of 59 Da and 15 Da because of successive loss of the decarboxylation and twice demethylations were observed in its negative MS^2 spectra. And its positive ion mode, the DPIs were *m/z* 179, 151, 123, and 108 *via* loss of H_2O, CH_2O_2, H_2O+2CO, and $CH_2O_2+CH_3$, respectively and based on the data, **M13** was putatively identified as dihydroferulic acid.

M15 was 2 Da more than CA and 14 Da less than **M13**. In the negative mode, it showed at *m/z* 181.0495$[M-H]^-$ ($C_9H_{10}O_4$, 2.6 ppm), and its NLFs of 44 Da and 15 Da (*m/z* 181→137→122) were observed in negative ESI-MS^2 spectrum. Similarly, its positive mode appeared a protonated ion at *m/z* 183.0652 ($C_9H_{10}O_4$, 0.1 ppm) with its elution time at 14.058 min and the DPIs were *m/z* 155 and 140 *via* loss of CO and $CO+CH_3$. Accordingly, we inferred that **M15** was the demethylated product of **M13**, and named as dihydrocaffeic acid. Metabolite **M18** gave rise to $[M+H]^+$ ion at *m/z* 209.1172 ($C_{12}H_{17}O_3$, 1.3 ppm) and $[M-H]^-$ ion at *m/z* 207.1027 ($C_{12}H_{17}O_3$, 0.2 ppm) at 14.516 min. It was 28 Da higher than CA, and engendered characteristic ions at *m/z* 181 $[M-C_2H_4]^+$ and *m/z* 135 $[M-C_2H_4-CO_2]^-$ in positive and negative ion mode, respectively. It was not hard to deduce that M18 was the demethylation product of CA, and we tentatively speculated it was 4-hydroxyphenyl-hexanoic acid.

DISCUSSION

Following analysis, it was demonstrated that CA could be metabolized to many small molecules, which suggested that CA was well biotransformation *in vivo*. Interestingly, CA metabolites, such as cinnamic acid, gallic acid and ferulic acid (FA) have biological activities similar to CA. **M5**, the methylated metabolite of CA, is FA, reduces the levels of inflammatory factors caused by Lipopolysaccharide (LPS), increased the antioxidant capacity and inactivated various mitogen-activated protein kinase signal pathway in lung, relieves symptoms in acute respiratory distress syndrome in rats [19]; and reduced the incidence of cardiovascular diseases *via* inhibition of oxidative stress, lipid peroxidation and inflammation by reduce the expression level of triglycerides and cholesterol, derivatives of reactive oxygen metabolites and tumor necrosis factor-alpha, respectively [20]. FA treatment for 4 weeks improved antioxidant enzymes levels, inhibited lipid peroxidation and expression of inflammatory mediators, reduced the astrocytic and microglial activation, suggesting that FA plays antioxidant and anti-inflammatory roles to alleviate Parkinson's disease [21]. In addition, FA treatment improves depression *via* hypothalamic-pituitary-adrenal axis in prenatally-stressed offspring rats [22]; improve learning and cognitive capacity *via* allaying the toxicity of β-amyloid to prevent Alzheimer's disease [23]. Furthermore, cinnamic acid (**M1**) has activities similar to CA. Cinnamic acid exerts antioxidant and anti-inflammatory activities and significantly improved learning cognition following traumatic brain injury and brain edema in rats [24]. Besides, dihydrocaffeic acid (DHCA, **M15**), the methylation product of CA, attenuated cell damage *via* reduced mitogen-activated protein kinase p38 single pathway phosphorylation, enhanced antioxidant enzymes activities and reduced production of lipid peroxidation, intracellular ROS and extracellular H_2O_2 [25]. It has also been shown that DHCA had a neuroprotective effect in cerebral edema and ischemic brain injury [26]. Moreover, both DHCA and dihydroferulic acid (**M13**) prevent the occurrence of cardiovascular disease *via* decreasing the platelet p-selectin expression and significantly enhancing fibrinogen binding on platelet [27]. Furthermore, 4-hydroxybenzoic acid (**M4**) reduces elevated production of ROS and nitric oxide induced by H_2O_2, meaningful and notable for the prevention and advance treatment of degenerative diseases of the nervous system [28]. Pretreatment with 3- (3-hydroxyphenyl) propionic acid (**M14**) and hippuric acid (**M9**) significantly inhibits osteoclast formation, suppresses osteoclastic cells restorative activity, and promoted body skeleton development [29].

Table 1: Summary of CA metabolites in rat biological samples

Peak	Ion Mode	t_R/min	Formula	Theoretical Mass m/z	Experimental Mass m/z	Error (ppm)	MS/MS Fragment Ions	Identification/ reactions	Identification/ reaction	P	U	F
M0	N	9.063	$C_9H_8O_4$	179.0339	179.0346	-2.1	134.0372, 135.0444	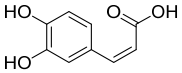	**prototype drug**		+	
	P	9.772	$C_9H_8O_4$	181.0859	181.0859	-0.1	91.0542, 135.0807, 137.0962, 153.0711, 163.0388				+	
M1	N	4.542	$C_9H_8O_2$	147.0441	147.0453	1.0	77.0391, 99.0088, 103.0541, 119.0519	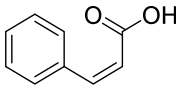	**cinnamic acid**	+		+
	P	4.542	$C_9H_8O_2$	149.0597	149.0594	-2.1	61.0287, 65.0389, 73.0662, 79.0543, 91.0536, 93.0328, 105.0721, 115.0536, 121.0292, 131.0504				+	+
M2	N	9.066	$C_8H_8O_2$	135.0451	135.0452	1.0	89.0238, 106.0404, 107.0510	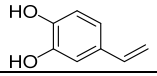	1,2-hydroxy-4-vinylbenzene		+	
M3	N	10.799	$C_{11}H_{13}NO_3$	206.0817	206.0826	1.6	58.0295, 70.0292, 72.0094, 91.0557, 103.0573, 121.9329, 147.0458, 164.0718	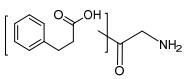	phenylpropionate -glycine			+
	P	6.245	$C_{11}H_{13}NO_3$	208.0968	208.0969	0.4	84.8598, 91.0558, 106.0646, 107.0485, 121.0642, 134.0595, 148.0769, 149.0591, 151.0638, 166.0858				+	
M4	N	7.425	$C_7H_6O_3$	137.0244	137.0238	4.5	81.0358, 93.0345, 108.0215, 136.0166	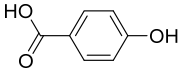	***p*-hydroxybenzoic acid**		+	+
M5	P	7.745	$C_{10}H_{10}O_4$	195.0653	195.0651	-1.0	79.0576, 95.0859, 107.0479, 115.1138, 131.0725, 133.0276, 136.0444, 139.1129, 160.0757, 163.0400, 167.0872, 180.0359, 186.0911	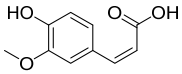	**ferulic acid**		+	

Table 2: Summary of CA metabolites in rat biological samples (*contd*)

Peak	Ion Mode	t_R/min	Formula	Theoretical Mass m/z	Experimental Mass m/z	Error (ppm)	MS/MS Fragment Ions	Identification/ reactions	Identification/ reaction	P	U	F
M6	N	8.255	$C_9H_8O_7S$	258.9918	258.9903	-5.8	96.9593, 107.0496, 125.0350, 134.0380, 135.0455, 153.0670, 179.0345	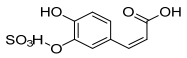	3-sulfonic-4-hydroxy-cinnamic acid		+	
M7	N	E	$C_{15}H_{16}O_{10}$	355.0671	355.0668	-0.8	71.0128, 85.0298, 112.9928, 113.0233, 135.0444, 149.0662, 161.0722, 175.0259, 179.0348, 190.0648, 205.0863, 219.0352, 249.0741, 269.1508, 311.0774	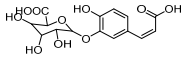	3-glucuronidation-4-hydroxy-cinnamic acid		+	
M8	P	8.530	$C_{10}H_{14}O_2$	167.0703	167.1067	0.3	55.0545, 67.0529, 69.0694, 79.0534, 81.0694, 84.9594, 91.0549, 97.1643, 95.0901, 105.0693, 107.0855, 109.1015, 123.0819, 149.0204	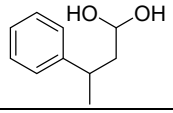	2-methyl-4-hydroxy-phenylpropionic acid		+	
M9	N	9.407	$C_9H_9NO_3$	178.0499	178.0510	1.3	108.0479, 134.0251, 135.0346, 149.0484, 151.0595, 160.0412	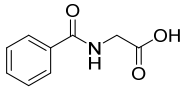	**hippuric acid**	+		+
M10	N	9.039	$C_{10}H_{10}O_7S$	273.0064	273.0077	0.9	133.0304, 134.0376, 137.0245, 149.0766, 178.0275, 193.0511	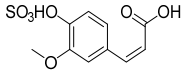	3-methoxy-4-sulfonic hydroxyl -cinnamic acid		+	
M11	N	9.304	$C_7H_6O_2$	121.0295	121.0296	0.8	92.0325, 93.0276, 95.0113, 108.0229	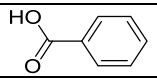	**benzoic acid**		+	+
	P	9.238	$C_7H_6O_2$	123.0441	123.0438	-2.1	51.0226, 53.03829, 67.0542, 77.0383, 95.0489		**benzoic acid**			+
M12	P	9.418	$C_9H_{10}O_2$	151.0754	151.0754	0.1	53.0375, 65.0391, 67.0534, 68.9799, 73.0467, 77.0381, 79.0553, 81.0684, 91.0542, 95.0493, 123.0821, 119.0483, 136.0527	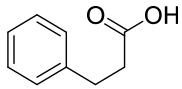	**3-phenylpropanoic acid**		+	+

Table 3: Summary of CA metabolites in rat biological samples (*contd*)

Peak	Ion Mode	t_R/min	Formula	Theoretical Mass m/z	Experimental Mass m/z	Error (ppm)	MS/MS Fragment Ions	Identification/ reactions	Identification/ reaction	P	U	F
M13	N	10.649	$C_{10}H_{12}O_4$	195.0652	195.0664	0.6	121.0286, 136.0543	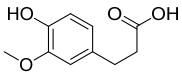	**dihydroferulic acid**			+
	P	9.108	$C_{10}H_{12}O_4$	197.0808	197.0814	2.9	55.0175, 65.0382, 73.0291, 77.0391, 108.0210, 117.0388, 123.0443, 125.1597, 149.0577, 151.0386, 179.0702				+	+
M14	N	10.735	$C_9H_{10}O_3$	165.0546	165.0548	1.1	106.0429, 119.0500, 119.0544, 121.0667	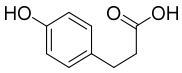	*p*-hydroxybenzene propanoic acid	+	+	+
	P	11.281	$C_9H_{10}O_3$	167.0703	167.0703	0.2	55.0550, 84.9589, 105.0691, 107.0521, 121.1011, 133.0173, 149.0463					+
M15	N	11.287	$C_9H_{10}O_4$	181.0495	181.0511	2.6	59.0143, 122.0390, 137.0639	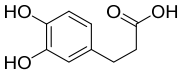	**dihydrocaffeic acid**			+
	P	14.058	$C_9H_{10}O_4$	183.0652	183.0652	0.1	56.9407, 67.0542, 83.0876, 95.085, 97.9687, 98.9844, 109.0275, 115.0526, 123.0430, 125.0220, 140.0461, 155.0690, 165.0692,				+	+
M16	P	11.334	$C_{11}H_{10}O_3$	191.0703	191.0699	-1.9	57.0697, 91.0534, 119.0867, 121.1006, 131.0881, 132.0556, 148.0518, 163.0763	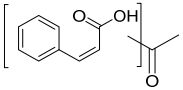	**cinnamic acid acetylate**		+	
M17	P	12.149	$C_{11}H_{12}O_3$	193.0859	193.0857	-1.1	55.0171, 67.0528, 77.0379, 81.0682, 91.0548, 95.0843, 105.0687, 109.1050, 119.0827, 133.1001, 147.0795, 151.0761, 157.0659, 175.1089	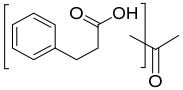	**3-phenylpropionate acetylate**		+	

Table 4: Summary of CA metabolites in rat biological samples (*contd*)

Peak	Ion Mode	t_R/min	Formula	Theoretical Mass m/z	Experimental Mass m/z	Error (ppm)	MS/MS Fragment Ions	Identification/ reactions	Identification/ reaction	P	U	F
M18	N	14.614	$C_{12}H_{16}O_3$	207.1016	207.1027	0.2	57.0342, 59.0140, 67.0560, 109.0654, 118.9930, 135.0841, 147.7209, 163.1118, 162.9853	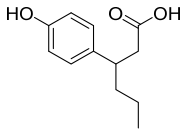	4-hydroxyphenyl-hexanoic acid		+	
	P	14.516	$C_{12}H_{16}O_3$	209.1172	209.1175	1.3	69.0362, 79.0541, 91.0525, 107.0842, 131.0928, 135.0807, 148.0893, 149.0965, 163.1105, 181.0870, 193.0032			+	+	
M19	N	14.907	$C_{11}H_{12}O_4$	207.0652	207.0663	0.1	132.0212, 133.0298, 134.0451, 135.0451, 161.0251, 179.0359	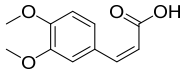	3,4-dimethoxycinnamic acid		+	
M20	N	15.170	$C_9H_8O_3$	163.0399	163.0404	2	91.0553, 101.0400, 117.0353, 163.0414	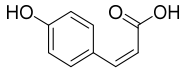	*p*-hydroxycinnamic acid			+
	P	20.751	$C_9H_8O_3$	165.0546	165.0547	0.5	67.0551, 77.0377, 95.0533, 109.0998, 123.0440, 137.0594, 147.0669				+	
M21	P	16.495	$C_8H_8O_3$	153.0546	153.0547	0.5	55.0540, 59.0508, 67.0538, 69.0703, 77.0381, 79.0536, 97.0653, 95.0852, 107.0874, 109.1027, 136.0383, 138.0316	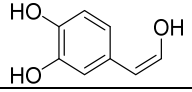	caffeic acid decarboxylation		+	

Note: t_R: retention time; P: plasma sample; U: urine sample; F: feces sample; +: existed

In a word, CA and its metabolites could exert antioxidant, anti-inflammatory and neuroprotective effects to cells or tissues. Therefore, further research can continue to study the metabolism of **M1** to **M21** *in vivo*. If these CA metabolites have a central substance that can be well absorbed and metabolized to most of the above structurally similar phenolic acids in the body, then human can concentrate on supplementing this compound instead of others, thus exert the great biological effects *in vivo*.

In the light of the chemical properties and functional groups of drug, we speculated its possible metabolites, when direct metabolites accumulate, it can also be metabolized by the body, and new metabolites are then generated. Due to the continuous drug metabolism reactions around the center gradually expand, all of the clustering center shall be carried out in accordance with the appropriate manner relationships, and eventually form the multiple drug metabolite clusters [30]. This method is applicable to the metabolism of most biologically active substances in the body. According to this approach, we listed the possible forms of CA metabolites, and combined UHPLC-Q-TOF mass spectrometer to rapidly screen CA metabolites *in vivo*, and quickly and effectively identified and demonstrated that CA mainly underwent methylation, decarbonylation, hydroxylation, hydrogenation and combined with sulfate and glucuronide, this discovery provides a theoretical basis for further research on the medicinal material basis of CA. However, the definite molecular mechanisms of which these metabolites work and the significance of the conversion between metabolites **M1** to **M21** and CA *in vivo* remain to be furtherly researched.

CONCLUSION

In this work, the metabolic mechanism of CA in rats' urine, plasma and feces was extended by analyzing compounds information, including retention time, EIC and the characteristic fragment ions in ESI-MS^2 spectrum, a total of 21 metabolites were identified under positive and negative ion mode, which could be of great significance to interpreting the biological activities and action mechanism of CA *in vivo*.

DECLARATIONS

Acknowledgement

This work was financially supported by "National Key R&D Program of China" (nos. 2018YFC1311400 and 2018YFC1311405), Premium Funding Project for Academic Human Resources Development in Beijing Union University (no. BPHR2017CZ03), Academic Research Projects of Beijing Union University (no. XP202007), Postgraduate Research Innovation Support Program of Beijing Union University (no. YZ2020K001), the Visiting scholar research project of Beijing Union University, and Beijing Key Laboratory of Bioactive Substances and Functional Foods, Beijing Union University (no. 12213991724010239).

Conflicts of interest

No conflict of interest associated with this work.

Contribution of authors

We declare that this work was done by the authors named in this article and all liabilities pertaining to claims relating to the content of this article will be borne by the authors. Yaxuan Sun and Jiayu Zhang conceived and designed the research; Yaxuan Sun, Jiayu Zhang, Shengquan Mi. and Jiaqi Yuan performed the UHPLC-Q-TOF mass spectrometry; Jiaqi Yuan, Yunting Wang, Yaxuan Sun and Shengquan Mi performed animal experiment; Jiaqi Yuan analyzed the date and completed the paper; all authors read and supported the final manuscript.

Open Access

REFERENCES

1. *Hung VP. Phenolic compounds of cereals and their antioxidant capacity. Crit Rev Food Sci Nutr 2016; 56(1): 25-35.*
2. *Fan Y, Piao CH, Hyeon E, Jung SY, Eom JE, Shin HS, Song CH, Chai OH. Gallic acid alleviates nasal inflammation via activation of Th1 and inhibition of Th2 and Th17 in a mouse model of allergic rhinitis. Int Immunopharmacol 2019; 70: 512-519.*
3. *Zhao DH, Wu YJ, Liu ST, Liu RY. Salvianolic acid B attenuates lipopolysaccharide-induced acute lung injury in rats through inhibition of apoptosis, oxidative stress and inflammation. Exp Ther Med 2017; 14(1): 759-764.*

4. Ebenezer O, Olaniyi O, Ayokanmi O, Oluwatobi A. Ameliorative Effect of Caffeic Acid on Capecitabine-Induced Hepatic and Renal Dysfunction: Involvement of the Antioxidant Defence System. Medicines 2017; 4(4): 78-80.
5. Espíndola KMM, Ferreira RG, Narvaez LEM, Rosario CRS, da Silva AHM, Silva AGB, Vieira APO, Monteiro MC. Chemical and Pharmacological Aspects of Caffeic Acid and Its Activity in Hepatocarcinoma. Front Oncol 2019; 9: 541-550.
6. Dziedzic A, Kubina R, Kabala-Dzik A, Wojtyczka RD, Morawiec T, Bułdak RJ. Caffeic Acid Reduces the Viability and Migration Rate of Oral Carcinoma Cells (SCC-25) Exposed to Low Concentrations of Ethanol. Int J Mol Sci 2014; 15(10): 18725-18741.
7. Jeon YD, Kee JK, Kim DS, Han YH, Kim SH, Kim SJ, Um JY, Hong SH. Effects of Ixeris dentata water extract and caffeic acid on allergic inflammation in vivo and in vitro. BMC Complement Altern Med 2015; 15(1): 196-206.
8. Huang X, Xi Y, Pan Q, Mao Z, Zhang R, Ma X, You H. Caffeic acid protects against IL-1β-induced inflammatory responses and cartilage degradation in articular chondrocytes. Biomed Pharmacother 2018; 107: 433-439.
9. Zhang Z, Wu X, Cao S, Wang L, Wang D, Yang H, Feng Y, Wang S, Li L. Caffeic acid ameliorates colitis in association with increased Akkermansia population in the gut microbiota of mice. Oncotarget 2016; 7(22): 31790–31799.
10. Agunloye OM, Oboh G. Modulatory effect of caffeic acid on cholinesterases inhibitory properties of donepezil. J Complement Integr Med 2017; 15(1): 1-10.
11. Liang G, Shi B, Luo W, Yang J. The protective effect of caffeic acid on global cerebral ischemia-reperfusion injury in rats. Behav Brain Funct 2015; 11(1): 18-27.
12. Li J, Bai Y, Bai Y, Zhu R, Liu W, Cao J, An M, Tan Z, Chang YX. Pharmacokinetics of Caffeic Acid, Ferulic Acid, Formononetin, Cryptotanshinone, and Tanshinone IIA after Oral Administration of Naoxintong Capsule in Rat by HPLC-MS/MS. Evid Based Complement Alternat Med 2017; 2017: 1-12.
13. Yaoyue L, Wenjing Z, Chenxiao W, Zijian W, Zhibin W, Jiayu Z. A comprehensive screening and identification of genistin metabolites in rats based on multiple metabolite templates combined with uhplc-hrms analysis. Molecules 2016; 23(8): 1862-1888.
14. Zhang JY, Wang ZJ, Li Y, Liu Y, Cai W, Li C, Lu JQ, Qiao YJ. A strategy for comprehensive identification of sequential constituents using ultra–High–performance liquid chromatography coupled with linear ion trap–Orbitrap mass spectrometer, application study on chlorogenic acids in Flos Lonicerae Japonicae. Talanta 2016; 147: 16-27.
15. Zhang J, Cai W, Zhou Y, Liu Y, Wu X, Li Y, Lu J, Qiao Y. Profiling and identification of the metabolites of baicalin and study on their tissue distribution in rats by ultra-high-performance liquid chromatography with linear ion trap-Orbitrap mass spectrometer. J Chromatogr B Analyt Technol Biomed Life Sci 2015; 985: 91-102.
16. Chen S, Li M, Zheng G, Wang T, Lin J, Wang S, Wang X, Chao Q, Cao S, Yang Z, Yu X. Metabolite Profiling of 14 Wuyi Rock Tea Cultivars Using UPLC-QTOF MS and UPLC-QqQ MS Combined with Chemometrics. Molecules 2018; 81(2): 321-338.
17. Penczynski KJ, Krupp D, Bring A, Bolzenius K, Remer T, Buyken AE. Relative validation of 24-h urinary hippuric acid excretion as a biomarker for dietary flavonoid intake from fruit and vegetables in healthy adolescents. Eur. J. Nutr. 2015, 56(2): 757-766.
18. Wu D, Wang H, Tan J, Wang C, Lin H, Zhu H, Liu J, Li P, Yin J. Pharmacokinetic and Metabolism Studies of Curculigoside C by UPLC-MS/MS and UPLC-QTOF-MS. Molecules 2018; 24(1): 21-34.
19. Zhang S, Wang P, Zhao P, Wang D, Zhang Y, Wang J, Chen L, Guo W, Gao H, Jiao Y. Pretreatment of ferulic acid attenuates inflammation and oxidative stress in a rat model of lipopolysaccharide-induced acute respiratory distress syndrome. Int J Immunopathol Pharmacol 2018; 32: 039463201775051-039463201775060.
20. Bumrungpert A, Lilitchan S, Tuntipopipat S, Tirawanchai N, Komindr S. Ferulic Acid Supplementation Improves Lipid Profiles, Oxidative Stress, and Inflammatory Status in Hyperlipidemic Subjects: A Randomized, Double-Blind, Placebo-Controlled Clinical Trial. Nutrients 2018; 10(6): 713-720.
21. Haque E, Javed H, Azimullah S, Khair SBA, Ojha S. Neuroprotective potential of ferulic acid in the rotenone model of Parkinson's disease. Drug Des Devel Ther 2015; 9: 5499-5510.
22. Heng X, Cheng Y, Chen Y, Yue Y, Li Y, Xia S, Li Y, Deng H, Zhang J, Cao Y. Ferulic Acid Improves Depressive-Like Behavior in Prenatally-Stressed Offspring Rats via Anti-Inflammatory Activity and HPA Axis. Int J Mol Sci 2019; 20(3): 493-509.
23. Yan JJ, Cho JY, Kim HS, Kim KL, Jung JS, Huh SO, Suh HW, Kim YH, Song DK. Protection against β-amyloid peptide toxicity in vivo with long-term administration of ferulic acid. Br J Pharmacol 2001; 133(1): 89-96.
24. Guo S, Zhen Y, Zhu Z, Zhou G, Zheng X. Cinnamic acid rescues behavioral deficits in a mouse model of traumatic brain injury by targeting miR-455-3p/HDAC2. Life Sci 2019; 235: 116819-116827.
25. De Oliveira MM, Ratti BA, Daré RG, Silva SO, Truiti MCT, Ueda-Nakamura T, Auzély-Velty R, Nakamura CV. Dihydrocaffeic Acid Prevents UVB-Induced Oxidative Stress Leading to the Inhibition of Apoptosis and MMP-1 Expression via p38 Signaling Pathway. Oxid Med Cell Longev 2019; 2019: 1-14.
26. Kyungjin L, Beom-Joon L, Youngmin B. Protective Effects of Dihydrocaffeic Acid, a Coffee Component Metabolite, on a Focal Cerebral Ischemia Rat Model. Molecules 2015; 20(7): 11930-11940.
27. Baeza G, Bachmair EM, Wood S, Mateos R, Bravo L, de Roos B. The colonic metabolites dihydrocaffeic acid and

dihydroferulic acid are more effective inhibitors of in vitro platelet activation than their phenolic precursors. Food Funct 2017; 8(3): 1333-1342.

28. *Winter AN, Brenner MC, Noelle P, Snodgrass M, Byars C, Arora Y, Linseman DA. Comparison of the neuroprotective and anti-inflammatory effects of the anthocyanin metabolites, protocatechuic acid and 4-hydroxybenzoic acid. Oxid Med Cell Longev 2017; 2017: 1-13.*
29. *Zhao H, Lazarenko OP, Chen JR. Hippuric acid and 3-(3-hydroxyphenyl) propionic acid inhibit murine osteoclastogenesis through RANKL-RANK independent pathway. J Cell Physiol 2020; 35(1): 559-610.*
30. *Yuqi W, Xiaodan Me, Zihan L, Jie L, Xiaoxin Z, Shuang L. Long D, Jiayu Z. Drug metabolite cluster-based data-mining method for comprehensive metabolism study of 5-hydroxy-6,7,3',4'-tetramethoxyflavone in rats. Molecules 2019; 24(18): 3278-3302.*